Published in final edited form as:
J Neuroimmunol. 2009 June 25; 211(1-2): 66–72. doi:10.1016/j.jneuroim.2009.03.015.

Viral nanoparticles associate with regions of inflammation and blood brain barrier disruption during CNS infection

Leah P. Shriver, **Kristopher J. Koudelka**, and **Marianne Manchester***
Department of Cell Biology and Center for Integrative Molecular Biosciences, The Scripps Research Institute, 10550 N. Torrey Pines Rd., La Jolla, CA 92037

Abstract

Targeted treatment of inflammatory diseases of the central nervous system (CNS) remains problematic due to the complex pathogenesis of these disorders and difficulty in drug delivery. The plant virus, cow pea mosaic virus (CPMV), has recently been explored as a nanoparticle delivery system for therapeutics targeting a number of diseases including cancer and neurodegeneration. To understand the biodistribution of CPMV in the CNS, we examined CPMV uptake during infection of mice with neurotropic mouse hepatitis virus (MHV). CPMV localized mainly to the CNS endothelium in areas that contained an intact blood brain barrier. However, in inflammatory lesions containing macrophage/microglial cell infiltration and IgG, CPMV could be detected in the brain parenchyma. Furthermore, CPMV showed rapid internalization in an *in vitro* model of the BBB. These results suggest that CPMV particles could be used to a vehicle to deliver therapeutics to the damaged CNS during neurodegenerative and infectious diseases of the CNS.

Keywords

CPMV; blood brain barrier; nanoparticles; microglial cells; central nervous system; targeting

1. Introduction

The use of viruses as nanoparticles has the potential to revolutionize targeted drug delivery and imaging technologies. A number of viruses are currently under study for their ability to be easily modified to carry drug cargos or to target specific tissues of the body (Muldoon et al., 1995; Raty et al., 2006). Delivery of drugs or gene therapy vectors to the central nervous system (CNS) has been particularly challenging.

Unlike peripheral organs, the CNS is protected from the diffusion of large particles from the circulation by the blood brain barrier (BBB). The BBB is composed of tight junctions consisting of integral transmembrane proteins; the claudins, occludins, and junctional adhesion molecules (Persidsky et al., 2006). In addition, CNS endothelial cells express multidrug resistant proteins, P-glycoprotein, and members of the ATP-binding cassette transporters that facilitate the elimination of drugs, toxins, and metabolites from the brain parenchyma (Loscher and Potschka, 2005). These mechanisms not only prevent the

*Corresponding author: 858 784 8086 858 784 7979 FAX marim@scripps.edu.

accumulation of toxic metabolites in the CNS, but also inhibit the effective treatment of diseases such as cancer and infection.

Several strategies using both viral and non-viral nanoparticles have been developed to aid in the delivery of therapies to the CNS. Silica nanoparticles, baculovirus, and TAT-conjugated polymers have all been used to target HIV drugs or gene therapy vectors to the brain (Bharali et al., 2005; Rao et al., 2008; Raty et al., 2006). However, the biodistibution of these particles varies greatly, and most show uptake by a limited number of cell types or must be administered directly into the brain.

The plant virus, CPMV, is a member of the genus *Comovirus* and is part of the *Picornaviridae* superfamily. CPMV is an attractive candidate for nanotechnology applications because of its excellent bioavailability. The virus is non-toxic even at high doses (up to 10^{16} particles/kg of body weight) and distributes to multiple organs after injection into animals (Rae et al., 2005; Singh et al., 2007). Reactive lysines and cysteines on the surface of the capsid can be conjugated to fluorescent dyes and metals such as gadolinium for use in imaging studies or peptide ligands for use in vaccine applications and targeted drug delivery (Destito et al., 2007; Lewis et al., 2006; McLain et al., 1996; Singh et al., 2007). These qualities make CPMV well-suited to manipulation as a nanoparticle for targeted *in vivo* delivery of therapeutics.

Previous work examining the biodistribution of CPMV nanoparticles after oral or intravenous administration into mice showed robust accumulation in the normal CNS by RT-PCR and by detection of fluorescently-labeled particles, even in perfused animals (Rae et al., 2005). In addition, CPMV has been shown to associate to the mammalian endothelium through an interaction a 54kD protein found on the surface of cells (Koudelka et al., 2007). However, it is unknown if CPMV interacts with endothelial cells of the CNS, and whether inflammatory conditions can affect its localization.

To study localization of CPMV in a model of CNS inflammation, we used mice infected with neurotropic mouse hepatitis virus (MHV) (Figure 1A). A member of the family *Coronaviridae*, MHV is an enveloped postitive-stranded RNA virus and commonly used as an animal model of the human demyelinating disease multiple sclerosis (MS) (Lane and Buchmeier, 1997). CNS infection of susceptible mouse strains with MHV results in an acute encephalomyelitis with breakdown of the BBB followed by a secondary inflammatory demyelinating phase characterized by damage to oligodendrocytes (Lane and Buchmeier, 1997; Zhou et al., 2003). Depending on the strain, MHV infects ependymal cells that line the ventricles, macrophages, microglia, astrocytes, and oligodendrocytes (Wang et al., 1992). Infectious virus is cleared approximately 2 weeks post-infection. However, the persistence of viral RNA in glial cells is thought to contribute the demyelination seen in the chronic phase of the disease due to infiltration of immune cells such as lymphocytes, macrophages, and activated microglial cells that results in tissue injury (Dandekar et al., 2004; Kim and Perlman, 2005; Lavi et al., 1984).

Understanding the interaction of viral nanoparticles with cells of the immune and central nervous systems during inflammatory diseases of the CNS is crucial to developing targeted drug delivery strategies for these disorders. MHV provides an easily manipulated model of CNS infection to test the *in vivo* targeting capability of CPMV. In this study, the association of CPMV with endothelial cells in the CNS was examined *in vivo* during intracerebral infection with MHV. In addition, uptake of CPMV was studied in bEND.3 cells, an *in vitro* model of the BBB, in order to establish if the uptake of CPMV occurs in the cerebral vasculature. Localization of CPMV in regions of BBB breakdown was examined in order to determine if CPMV could be targeted to other CNS cell types during inflammation.

2. Materials and Methods

Mice

Adult female C57BL/6 mice were obtained from the rodent breeding colony maintained by the Scripps Research Institute (La Jolla, CA) and housed according to institutional animal care and use committee (IACUC) guidelines.

Infection of Mice with MHV and plaque assay

MHV strain JHM was kindly provided by Dr. Thomas Lane (University of California, Irvine). Virus stocks were grown in 17CL1 cells as follows. Cells were infected at a MOI of 0.1 for approximately 5 hours followed by the addition of new media. Infection was allowed to proceed for 18 hours until cells lifted off the sides of the flask. Supernatant was removed and spun at 1500 rpm at 4°C for 10 minutes. Stocks were titered on DBT cells by plaque assay as previously described (Lane et al., 2000). C57BL/6 mice received one intracranial inoculation of 50 PFU MHV diluted in sterile PBS to a final volume of 30 μl. Control mice received one inoculation of sterile PBS in a final volume of 30 μl. Following infection, mice were monitored for clinical symptoms. Disease was scored as follows 1=waddling gait, hunched, 2=hind limb paresis, 3=hind limb paralysis, 4=hind and forelimb paralysis, and 5=moribund. Plaque assays were performed on brain, spinal cord, and liver as previously described (Lane et al., 2000).

Purification and Labeling of CPMV

CPMV was grown in California Blackeye 5 plants obtained from The Burpee Company. Plants were grown and mechanically inoculated with wild-type CPMV. Purified CPMV was prepared as previously described (Khor et al., 2002) and labeled with alexa fluor 555 (AF555). To conjugate AF555 dyes to lysines on wild-type CPMV capsid, 1 mg AF555 carboxylic acid, 2,3,5,6-tetrafluorophenyl ester (Invitrogen, Carlsbad, CA) was suspended in 0.1 M K-phosphate buffer and mixed with 5 mg of CPMV in a total volume of 2.5 ml using a molar ratio of 10 dyes per asymmetric unit. The virus-dye suspension was incubated overnight at room temperature in a rolling shaker. After incubation the samples were initially purified by ultracentrifugation at 42,000 rpm (3 hours, 4°C) and resuspended in 1 ml of the same buffer. To eliminate free dye the sample was further purified by sucrose gradient (10%-40% w/v in PBS) ultracentrifugation at 28,000 rpm (3 hours, 4°C). After collecting the labeled CPMV fraction the virus was concentrated by ultracentrifugation at 42,000 rpm (3 hours, 4°C). The final pellet was resuspended in PBS (Gibco-BRL) and filtered through a 0.2-μm membrane (Costar) to eliminate aggregate particles and sterilize the sample. Particles were examined by FPLC on a Superose™-6 size-exclusion column (Amersham Pharmacia). The number of dyes per particle was calculated where dyes/particle = $[(Abs_{260} \times \text{dilution}) / \in_{AlexaFluor\ 555}] / (\text{concentration of CPMV} / \text{molecular weight of CPMV})$; where $\in_{AlexaFluor\ 555} = 150{,}000$ and the molecular weight of CPMV = 5.6×10^6grams/mole.

Immunohistochemistry and fluorescence confocal microscopy

On days 3, 7, and 10 after MHV infection, three mice per timepoint were administered 100 μg of alexa fluor 555 labeled CPMV (CPMV-A555). One hour later mice were deeply anesthetized and intracardially perfused with ice cold PBS. Brain and spinal cord were dissected, frozen in OCT mounting medium (Tissue Tek, Torrence, CA), and 10 μm cryosections were prepared. Sections were stained with alexa fluor 488 conjugated anti-mouse IgG (BD Biosciences), FITC conjugated CD11b (ebiosciences, San Diego, CA), anti-CD31 (BD Biosciences) and anti-claudin 5 (Invitrogen, Carlsbad, CA) followed by an alexa fluor 488 conjugated anti-mouse IgG_1. Images were taken with the The Bio-Rad (Zeiss)

Radiance 2100 Rainbow laser scanning confocal microscope (Hercules, CA) and Image J analysis software.

Uptake of CPMV by bEND. 3 cells

. bEND.3 cells (ATCC, Manassas, VA) were cultured in DMEM supplemented with 10% fetal bovine serum and penicillian/streptomycin (Invitrogen, Carlsbad, CA) in Lab-Tek chamber slides (Nalge Nunc, Rochester, NY). Unlabeled CPMV was added to the cells at a concentration of 10^5 virus particles/cell and incubated at 37°C for 1-3 hours. Cells were fixed with 95% ethanol, blocked in 10% normal goat serum (Sigma, St. Louis, MO), and stained with anti-CPMV polyclonal antibody followed by an alexa fluor 555 conjugated rabbit IgG. In addition, cells were stained with anti-claudin 5 antibody and imaged.

Hematoxylin and Eosin Staining. Frozen sections from mock-infected and MHV-infected mice were fixed in 4% paraformaldehyde (EM Sciences, Hatfield, PA). Slides were stained with hematoxylin (Vector Labs, Burlingame, CA), washed in water, and subsequently dehydrated in 50%, and 75% ethanol. Sections were stained in eosin (Sigma, St. Louis, MO), and washed in 95% and 100% ethanol followed by a clearing step in Accustain (Sigma, St. Louis, MO). Sections were mounted with VectaMount (Vector Labs, Burlingame, CA), followed by brightfield imaging on a Nikon Eclipse TS100 microscope.

3. Results

CPMV shows the ability to bind to and be internalized by endothelial cell lines, and was detected in brain homogenates after i.v. inoculation into wildtype mice (Koudelka et al., 2007; Rae et al., 2005). However, it was unknown whether CPMV could specifically interact with the specialized cells of the blood brain barrier. To characterize the interaction with brain endothelial cells, the uptake of CPMV by the mouse brain endothelial cell line, bEND.3 was studied *in vitro*. bEND.3 cells display many characteristics of the blood brain barrier such as transendothelial resistance and expression of claudin-5 (Figure 1A and (Koto et al., 2007)). Purified CPMV was added to bEND.3 cells at a concentration of 10^5 virus particles/cell and incubated for 1 hour at 37°C, conditions previously shown to promote internalization by CPMV (Lewis et al., 2006). Robust binding and internalization of CPMV was seen in these cells after performing immunohistochemistry with an anti-CPMV antibody (Figure 1A, B). After internalization, CPMV has a perinuclear distribution indicating uptake by endocytic vesicles, similar to the distribution previously observed in fibroblasts (Lewis et al., 2006) (Figure 1C).

We next examined whether this particle could associate with endothelial cells of the BBB *in vivo*, during normal and disease states in mice. To establish a model of neuroinflammation and BBB breakdown, MHV infection of mice was employed. C57BL/6 mice are susceptible to infection with neurotropic MHV and develop encephalitis followed by an inflammatory demyelinating disease that resembles MS (Figure 2A). Mice were infected with a single intracerebral (i.c.) inoculation containing 50 PFU of MHV and the disease course was compared with mock infected mice that received an equal volume of PBS i.c. Symptoms in MHV infected mice appeared approximately day 3 after infection, and rapidly progressed so that a majority of mice showed limb paralysis by day 6 after infection (Figure 2B). Typically complete clearance of virus in the CNS and periphery is observed by two weeks post-infection (Lane and Buchmeier, 1997). After MHV infection, mice displayed infiltration of inflammatory cells throughout the brain paraenchyma and in brain meninges indicating that the virus elicited a robust inflammatory response in the CNS (Figure 2C and data not shown).

We examined the distribution of CPMV in cerebral endothelial cells in normal mice and during CNS infection with MHV to determine whether localization to endothelial cells occurred in normal brain or during CNS inflammation. CPMV particles were labeled with alexa fluor 555 (AF555) dye via N-hydroxysuccinimide ester chemistry (Figure 3A). The NHS ester group reacts with lysines on the viral capsid, resulting in the covalent attachment of dyes to the surface of the viral particle to generate CPMV-AF555 (Lewis et al., 2006; Wang et al., 2002). Labeled CPMV-AF555 particles were purified and subsequently analyzed by size exclusion FPLC on a Sepharose 6 column (Figure 3B). The fluorescence peak coeluted with CPMV particles, indicating specific labeling of CPMV. The attachment efficiency was calculated at approximately 30 AF555 dyes/particle (Figure 3 and (Lewis et al., 2006)).

CPMV-AF555 (100 μg/mouse) was injected intravenously into mock-infected or MHV-infected mice on days 3, and 10 post-MHV infection, and mice were sacrificed 30 minutes after the CPMV injection. Healthy mice showed localization of punctuate CPMV-A555 signal in CD31-positive endothelial cells in meninges and brain parenchyma, similar to the endothelial distribution seen in other organs after CPMV-A555 injection into mice (Figure 4 A,D, G, J and (Lewis et al., 2006)and Koudelka submitted). This endothelial localization was similar during MHV infection (Figure 4 B, C, E, F, H, and I), in particular in vessels that continued to express claudin-5, one of the main proteins localized to tight junctions in the BBB (Figure 4L) (Huber et al., 2001). However, in contrast to mock infection, CPMV-A555 particles were also observed outside of CD31 positive vessels in the MHV-infected mice (Figure 4H, I). Fluorescence signal was quantified inside and outside the vessel. Similar levels of CPMV were seen in vessels in both mock-infected and MHV-infected mice. However after MHV infection, approximately 25% of the fluorescence signal is located outside the vessel (Supplementary Figure 1). Therefore, it appears that CPMV can penetrate the BBB and it may be possible that additional CNS cell types take up CPMV in the brain parenchyma during infection.

During MHV infection, CPMV-AF555 particles were observed outside CNS vessels, suggesting leakage of CPMV across the BBB. Therefore, the localization of CPMV was examined in regions where BBB disruption was evident. In order to detect BBB breakdown, brain and spinal cords of MHV infected mice were stained with antibodies to mouse IgG, which cannot normally penetrate a healthy BBB. Mock infected mice showed no evidence of IgG in the brain parenchyma or BBB breakdown, while MHV infected mice had a diffuse distribution of IgG in the brain parenchyma (Figure 5). Regions that contained an influx of IgG also showed localization of CPMVAF555 particles (Figure 5).

The breakdown of the BBB during MHV infection is typically accompanied by infiltration of immune cells and activation of microglia. Macrophages and microglia have the ability to phagocytose viruses and bacteria during inflammatory conditions. Therefore, we examined whether CPMV-AF555 localization occurred in lesions containing macrophages and microglia, and whether there was CPMV uptake by these cells. CPMV-AF555 particles were observed in regions that contained macrophages and microglial cells as seen by positive staining with the antibody specific for CD11b. In addition, some colocalization was also observed between CPMV particles and $CDllb^{+}$ microglial cells. These cells had a stellate morphology, which distinguished them from peripheral macrophages (Figure 5K). These data indicate that CPMV can penetrate the BBB and target inflammatory lesions directly.

4. Discussion

The plant virus CPMV has been used for biomedical applications such as drug targeting, vaccines, delivery, and vascular imaging (Destito et al., 2007; Lewis et al., 2006; McLain et al., 1996). The versatility of this nanoparticle is due to its ease of production, lack of toxicity, and the ability to manipulate the particle chemically and genetically. In this study, the localization of CPMV in CNS tissue was examined in healthy animals or during infection with neurotropic MHV. Examination of the CNS by confocal microscropy showed that injection of CPMV into mice with MHV infection results in uptake by cerebral endothelial cells. However, breakdown of the BBB facilitated the movement of CPMV out of the vasculature and into the brain parenchyma, specifically in lesions that contained infiltrating immune cells.

In order to confirm the localization of CPMV in brain endothelial cells, CPMV uptake was measured in the mouse brain endothelial cell line, bEND.3. These cells form tight junctions and express proteins such as claudin-5 (Koto et al., 2007). Previous work has shown that after uptake CPMV localizes primarily to the late endosomal compartment (Lewis et al., 2006). This is consistent with the primarily perinuclear distribution of CPMV in the bEND.3 cells. Therefore, these cells provide an in vitro model to study conditions that affect CPMV uptake at the blood brain barrier.

MHV infection provides an ideal model to study the interaction of CPMV during inflammation-mediated BBB breakdown *in vivo*. Mice showed symptoms by day 3 after infection, which corresponds to active replication of virus in the CNS. By day 10 mice displayed limb paralysis, a time point where virus is typically cleared from the parenchyma and inflammatory cells were detected. Therefore, the distribution of CPMV particles could be observed during an active virus infection in the CNS as well as later in the disease course when the pathology is primarily mediated by the immune system.

The distribution of nanoparticles *in vivo* depends on properties intrinsic to the virus such as surface charge, size, and the interaction of viral proteins with molecules expressed on cells. The method of administration also determines targeting of nanoparticles to different tissues in the body. A number of particles have been tested for their ability to interact with cells of the CNS. Stereotactic injection of iron oxide conjugated baculovirus into rat brain ventricles results in the localization of particles in cells of the choroid plexus (Raty et al., 2006). Cationic albumin-conjugated pegylated nanoparticles accumulated in the periventricular region and 3rd ventricle after intravenous injection into mice (Lu et al., 2005). In both these instances, the increased permeability of the ventricular region may have facilitated delivery of the nanoparticles. In contrast to the primarily ventricular distribution of the previous particles, adenovirus and herpesvirus particles showed uptake by neuronal cells. However, in these studies osmotic disruption or direct injection into the CNS was necessary to cross the BBB (Muldoon et al., 1995). In this study, CPMV efficiently targeted cells of the cerebral vasculature after peripheral administration. During mock infection, CD31 positive vessels show accumulation of labeled CPMV particles. A similar distribution pattern is seen on days 3 and 10 after MHV infection. CPMV accumulates in endothelial cells throughout the meninges and in the CNS parenchyma in both mock infected and MHV infected mice.

The ability of CPMV to specifically target the CNS vasculature may allow specific delivery of molecules that decrease endothelial cell permeability. A number of neurodegenerative and infectious diseases such as multiple sclerosis, amyotrophic lateral sclerosis, and HIV encephalitis show early disruption of the BBB that may contribute to disease symptoms (Kanmogne et al., 2007; Persidsky et al., 2006). The conjugation of CPMV with drugs or

molecules that target BBB dysfunction could potentially protect the CNS from nonspecific damage that occurs due to leakage of molecules from the circulation.

Despite widespread localization of CPMV to the vasculature during MHV infection, it was evident that CPMV was also able to cross the BBB and enter into the CNS parenchyma. CPMV localizes to areas where IgG and inflammatory cells are present, specifically in regions of BBB breakdown. In addition, a subset of particles is taken up by resident microglial cells. Since CPMV is capable of crossing the BBB during injury, future studies will determine if chemical modification of the CPMV capsid may facilitate uptake by additional CNS resident cells such as neurons and oligodendrocytes. Neurotrophic factors have shown efficacy in animal models of neurodegenerative and demyelinated diseases, but appear not to cross the BBB effectively (Suzuki and Svendsen, 2008). Empty CPMV particles could potentially be loaded with neurotrophic factors and targeted to neuronal or glial cells through modification of the CPMV capsid, providing an efficient delivery system for these factors.

In summary, this study shows that CPMV localizes to both endothelial cells in normal brain, but during infection virus crosses the BBB where it is taken up by CNS resident microglial cells. CPMV has the ability to target multiple cell types during CNS inflammation. This makes it an attractive candidate nanoparticle to shuttle therapeutics into the CNS during inflammatory conditions.

Supplementary Material

Refer to Web version on PubMed Central for supplementary material.

References

Bharali DJ, Klejbor I, Stachowiak EK, Dutta P, Roy I, Kaur N, Bergey EJ, Prasad PN, Stachowiak MK. Organically modified silica nanoparticles: a nonviral vector for in vivo gene delivery and expression in the brain. Proc Natl Acad Sci U S A 2005;102:11539–11544. [PubMed: 16051701]

Dandekar AA, Anghelina D, Perlman S. Bystander CD8 T-cell-mediated demyelination is interferon-gamma-dependent in a coronavirus model of multiple sclerosis. Am J Pathol 2004;164:363–369. [PubMed: 14742242]

Destito G, Yeh R, Rae CS, Finn MG, Manchester M. Folic acid-mediated targeting of cowpea mosaic virus particles to tumor cells. Chem Biol 2007;14:1152–1162. [PubMed: 17961827]

Huber JD, Egleton RD, Davis TP. Molecular physiology and pathophysiology of tight junctions in the blood-brain barrier. Trends Neurosci 2001;24:719–725. [PubMed: 11718877]

Kanmogne GD, Schall K, Leibhart J, Knipe B, Gendelman HE, Persidsky Y. HIV-1 gp120 compromises blood-brain barrier integrity and enhances monocyte migration across blood-brain barrier: implication for viral neuropathogenesis. J Cereb Blood Flow Metab 2007;27:123–134. [PubMed: 16685256]

Khor IW, Lin T, Langedijk JP, Johnson JE, Manchester M. Novel strategy for inhibiting viral entry by use of a cellular receptor-plant virus chimera. J Virol 2002;76:4412–4419. [PubMed: 11932408]

Kim TS, Perlman S. Viral expression of CCL2 is sufficient to induce demyelination in RAG1-/- mice infected with a neurotropic coronavirus. J Virol 2005;79:7113–7120. [PubMed: 15890951]

Koto T, Takubo K, Ishida S, Shinoda H, Inoue M, Tsubota K, Okada Y, Ikeda E. Hypoxia disrupts the barrier function of neural blood vessels through changes in the expression of claudin-5 in endothelial cells. Am J Pathol 2007;170:1389–1397. [PubMed: 17392177]

Koudelka KJ, Rae CS, Gonzalez MJ, Manchester M. Interaction between a 54-kilodalton mammalian cell surface protein and cowpea mosaic virus. J Virol 2007;81:1632–1640. [PubMed: 17121801]

Lane TE, Buchmeier MJ. Murine coronavirus infection: a paradigm for virus-induced demyelinating disease. Trends Microbiol 1997;5:9–14. [PubMed: 9025229]

Lane TE, Liu MT, Chen BP, Asensio VC, Samawi RM, Paoletti AD, Campbell IL, Kunkel SL, Fox HS, Buchmeier MJ. A central role for CD4(+) T cells and RANTES in virus-induced central nervous system inflammation and demyelination. J Virol 2000;74:1415–1424. [PubMed: 10627552]

Lavi E, Gilden DH, Highkin MK, Weiss SR. Persistence of mouse hepatitis virus A59 RNA in a slow virus demyelinating infection in mice as detected by in situ hybridization. J Virol 1984;51:563–566. [PubMed: 6086966]

Lewis JD, Destito G, Zijlstra A, Gonzalez MJ, Quigley JP, Manchester M, Stuhlmann H. Viral nanoparticles as tools for intravital vascular imaging. Nat Med 2006;12:354–360. [PubMed: 16501571]

Loscher W, Potschka H. Role of drug efflux transporters in the brain for drug disposition and treatment of brain diseases. Prog Neurobiol 2005;76:22–76. [PubMed: 16011870]

Lu W, Zhang Y, Tan YZ, Hu KL, Jiang XG, Fu SK. Cationic albumin-conjugated pegylated nanoparticles as novel drug carrier for brain delivery. J Control Release 2005;107:428–448. [PubMed: 16176844]

McLain L, Durrani Z, Wisniewski LA, Porta C, Lomonossoff GP, Dimmock NJ. Stimulation of neutralizing antibodies to human immunodeficiency virus type 1 in three strains of mice immunized with a 22 amino acid peptide of gp41 expressed on the surface of a plant virus. Vaccine 1996;14:799–810. [PubMed: 8817828]

Muldoon LL, Nilaver G, Kroll RA, Pagel MA, Breakefield XO, Chiocca EA, Davidson BL, Weissleder R, Neuwelt EA. Comparison of intracerebral inoculation and osmotic blood-brain barrier disruption for delivery of adenovirus, herpesvirus, and iron oxide particles to normal rat brain. Am J Pathol 1995;147:1840–1851. [PubMed: 7495307]

Persidsky Y, Ramirez SH, Haorah J, Kanmogne GD. Blood-brain barrier: structural components and function under physiologic and pathologic conditions. J Neuroimmune Pharmacol 2006;1:223–236. [PubMed: 18040800]

Rae CS, Khor IW, Wang Q, Destito G, Gonzalez MJ, Singh P, Thomas DM, Estrada MN, Powell E, Finn MG, Manchester M. Systemic trafficking of plant virus nanoparticles in mice via the oral route. Virology 2005;343:224–235. [PubMed: 16185741]

Rao KS, Reddy MK, Horning JL, Labhasetwar V. TAT-conjugated nanoparticles for the CNS delivery of anti-HIV drugs. Biomaterials 2008;29:4429–4438. [PubMed: 18760470]

Raty JK, Liimatainen T, Wirth T, Airenne KJ, Ihalainen TO, Huhtala T, Hamerlynck E, Vihinen-Ranta M, Narvanen A, Yla-Herttuala S, Hakumaki JM. Magnetic resonance imaging of viral particle biodistribution in vivo. Gene Ther 2006;13:1440–1446. [PubMed: 16855615]

Singh P, Prasuhn D, Yeh RM, Destito G, Rae CS, Osborn K, Finn MG, Manchester M. Bio-distribution, toxicity and pathology of cowpea mosaic virus nanoparticles in vivo. J Control Release 2007;120:41–50. [PubMed: 17512998]

Suzuki M, Svendsen CN. Combining growth factor and stem cell therapy for amyotrophic lateral sclerosis. Trends Neurosci 2008;31:192–198. [PubMed: 18329734]

Wang FI, Hinton DR, Gilmore W, Trousdale MD, Fleming JO. Sequential infection of glial cells by the murine hepatitis virus JHM strain (MHV-4) leads to a characteristic distribution of demyelination. Lab Invest 1992;66:744–754. [PubMed: 1318460]

Wang Q, Kaltgrad E, Lin T, Johnson JE, Finn MG. Natural supramolecular building blocks. Wild-type cowpea mosaic virus. Chem Biol 2002;9:805–811. [PubMed: 12144924]

Zhou J, Stohlman SA, Hinton DR, Marten NW. Neutrophils promote mononuclear cell infiltration during viral-induced encephalitis. J Immunol 2003;170:3331–3336. [PubMed: 12626593]

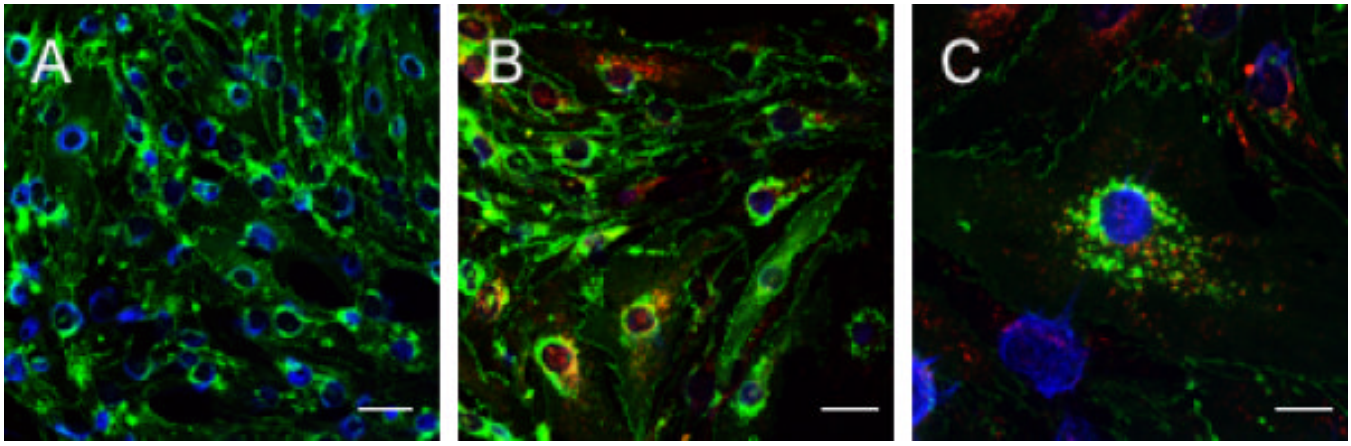

Figure 1.

CPMV uptake in bEND.3 cells. A) mock infected bEND.3 cells stained with antibody to CPMV followed by A555 conjugated rabbit IgG and anti-claudin-5 antibody and A488 conjugated mouse IgG_1 secondary. B & C) bEND.3 cells incubated with 10^5 virus particles/cell and stained with anti-CPMV and anti-claudin-5 (magnification is 200x, scale bar=40 microns). C) magnification is 600x, scale bar=80 microns. Green = claudin-5, red = CPMV, and blue = DAPI.

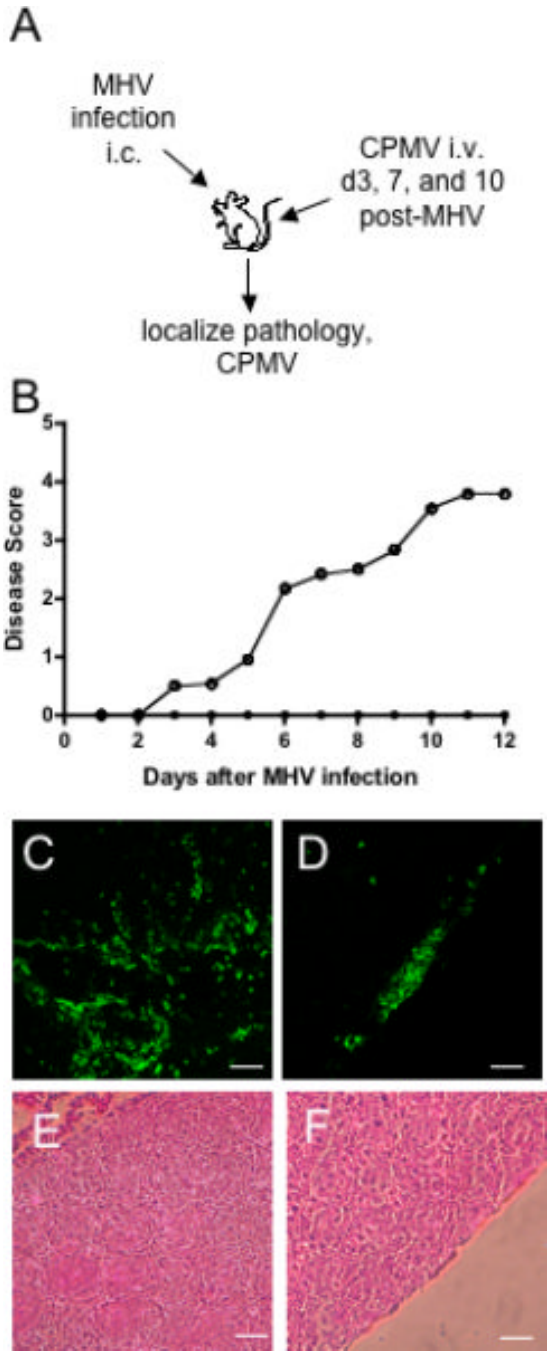

Figure 2.

Disease course during CNS infection with MHV. A) Experimental design for MHV infection and CPMV administration in mice. B) Average disease score for 10 mice intracerebrally inoculated with 30 μl MHV strain JHM diluted in sterile PBS (○) and 10 mice receiving an equal volume of PBS as a control (•). Immunohistochemical examination of MHV pathology with FITC-conjugated anti- CDllb antibody. Prominent infiltration of $CD11b^+$ cells (green) in the brain parenchyma (C) and throughout the meninges (D) are seen after MHV infection. E & F) Hematoxylin and eosin staining during MHV infection. Infiltrating immune cells are located near the lateral ventricle , brain parenchyma, and meninges.

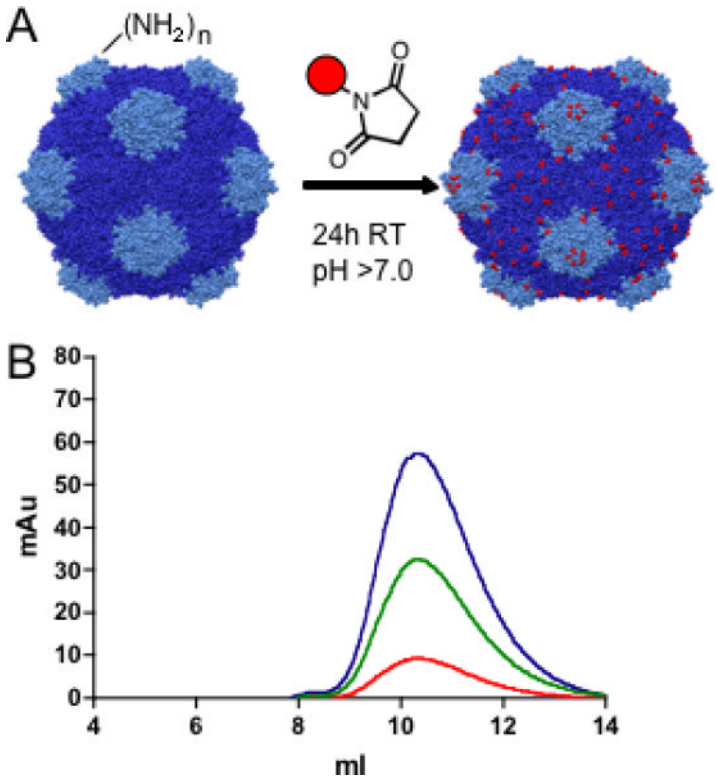

Figure 3.

Attachment of Alexa fluor 555 to CPMV. Schematic of N-hydroxysuccinimide ester chemistry. A) The NHS reacts with lysines on the viral capsid resulting in the attachment of dyes to the surface of the viral particle. B) Size exclusion FPLC analysis of CPMV-A555 particles. The fluorescence peak for alexa fluor 555 (555 nm-red) coelutes with the viral particles protein content (280nm-green) and nucleic acid content (260nm-blue) indicating specific labeling of intact CPMV particles.

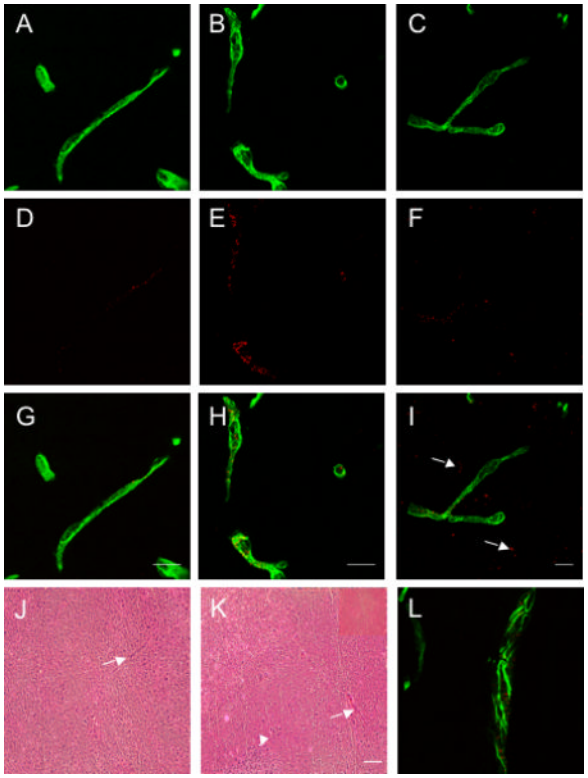

Figure 4.
CPMV localizes to endothelial cells in the cerebral vasculature. Confocal images of CD31 positive vessels from the brains of mock infected (A), and MHV infected mice on days 3 (B) and 10 (C). CPMV-A555 fluorescence in mock infected mice (D) and days 3 (E) and 10 (F) after MHV infection. G-I) Merged images of CPMVA555 and CD31 from mock infected and MHV infected mice. Arrows indicate regions where CPMV has penetrated into the brain parenchyma. J) Merged image of claudin-5 staining and CPMV-A555 on day 10 after MHV infection. Scale bar is 15 microns and magnification is 600x for all images. Images are representative of three mice examined at each timepoint. J & K) H & E stain of brain after mock infection and MHV infection. Arrows indicate blood vessels in tissue and arrowhead is a region containing inflammatory infiltrates. (Magnification is 100x and scale bar is 50 microns). Inset is a blood vessel at 200x magnification.

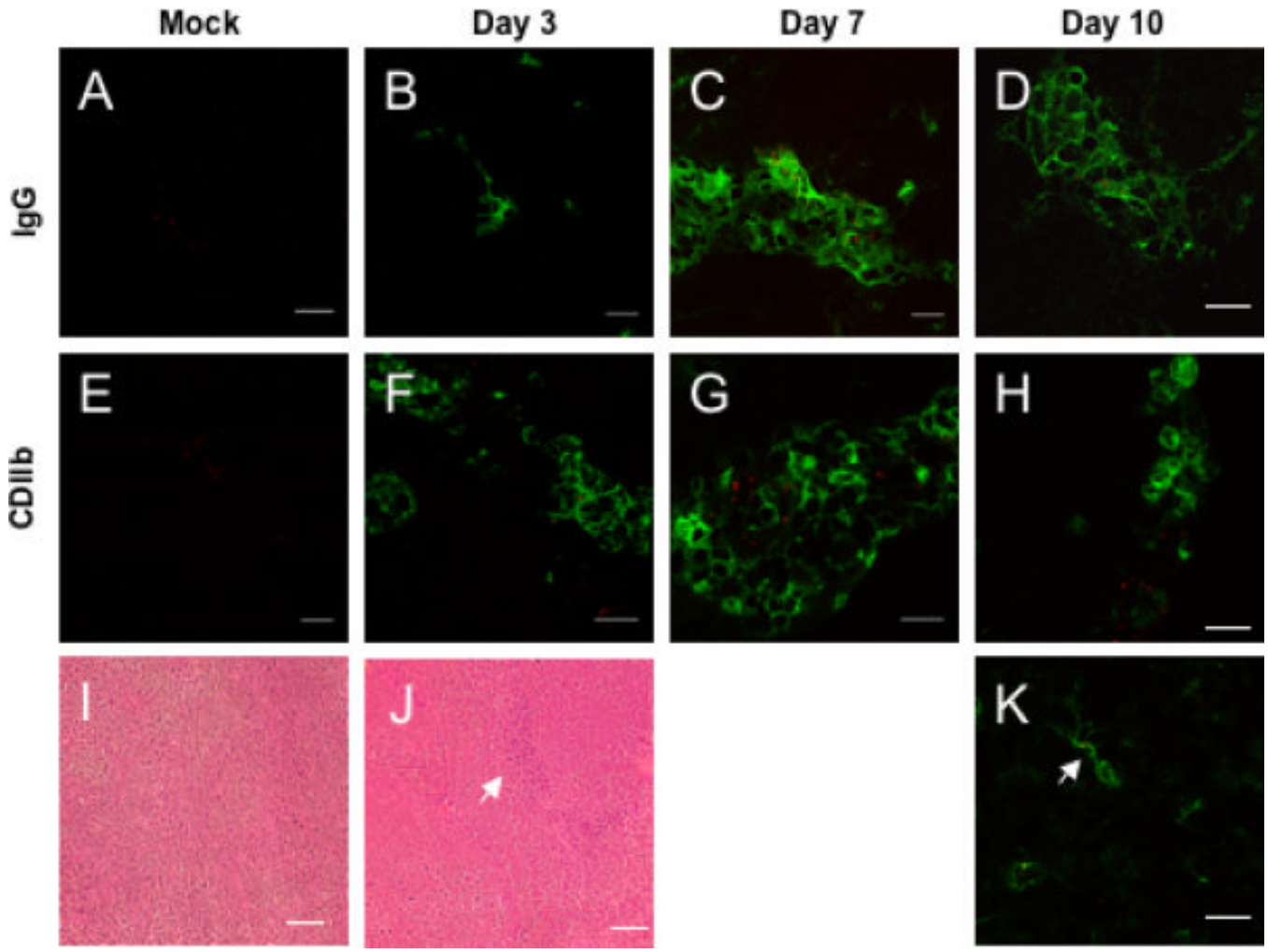

Figure 5.

CPMV penetrates the BBB during CNS infection. A-D) Fluorescence immunohistochemistry with A488 conjugated anti-mouse IgG in the brains of mock infected mice and on days 3, 7, and 10 after MHV infection. E-I) FITC conjugated anti-CD11b staining in mouse brains after mock infection and days 3, 7, and 10 after intracerebral inoculation with MHV. Red = CPMV. $CDllb^{+}$ microglial cells exhibit a characteristic stellate morphology and arrow indicates colocalization of a microglial cell with CPMV (I). Magnification is 600x and scale bar is 15 microns. H &E staining of brain parenchyma from mock-infected (I) and MHV-infected (J) mice. Arrow indicates inflammatory cells within the tissue. Images are representative of three mice examined at each timepoint.